To appear in the *International Journal of Electronics*
Vol. 00, No. 00, Month 20XX, 1–23

Prediction of Subharmonic Oscillation in Switching Regulators: From a Slope to a Ripple Standpoint

A. El Aroudi[a*], M. Al-Numay[b], J. Calvente[a], R. Giral[a], E. Rodriguez[c] and E. Alarcn[c]

[a] *Departament d'Enginyeria Electrnica, Elctrica i Automtica, of Universitat Rovira i Virgili, Tarragona, Spain*

[b] *Electrical Engineering Department, King Saud University, Riyadh, KSA*

[c] *Department of Electronics Engineering at BarcelonaTech (UPC)*, Barcelona, Spain

(*v4.1 released September 2014*)

New exact critical conditions for predicting subharmonic instability in switching regulators are approximated by simple design-oriented expressions valid under practical conditions. These simplified expressions contain the ripple and slope information of the feedback control signal. Depending on the converter topology, the controller used and values of parasitic parameters, either the slope or the ripple can be dominant in predicting instability. A discussion on the validity of this interpretation is illustrated through six different examples of switching regulators using the concept of the spectral radius and the relative degree of the system loop. Using this approach, The boundary between the desired stable region and the subharmonic instability can be easily obtained. The theoretical results are validated by means of numerical simulations.

Keywords: DC-DC converters, subharmonic oscillation, stability.

1. Introduction

Switch mode operation of power converters is carried out by means of Pulse Width Modulation (PWM) action on the switching semiconductor devices. In analog Voltage Mode Control (VMC), known also as duty cycle control, the fixed frequency square wave PWM signal is generated by obtaining the output error voltage, processing it by a suitable controller hence obtaining the control signal $v_{\rm con}(t)$ and comparing the result with a periodic ramp signal $v_{\rm ramp}(t)$ (Erickson and Maksimovic , 2001; Middlebrook and Čuk , 1977). In most applications trailing edge modulation is used in which the square wave signal $u(t)$ driving the main switch of the converter is high when the control signal $v_{\rm con}(t)$ is higher than the ramp signal $v_{\rm ramp}(t)$ and is low in the opposite case. Hence the ramp signal is this modulation strategy is fed to the negative input of the comparator while the error voltage is fed to its non-inverting input. In Current Mode Control (CMC), the switch is turned ON periodically by using a cloked S-R latch while it is turned OFF whenever the sensed inductor current reaches a reference signal dictated by the outer voltage loop. It is

*Corresponding author. abdelali.elaroudi@urv.cat

worth noting that a converter under CMC generally uses the inductor current, as well as the output voltage error signal, as input signals to the modulator and hence to generate the driving signal $u(t)$. CMC is one of the most popular techniques used in DC-DC switched regulators due to its superiority as compared to VMC Deisch (1978); Lee (2014); Tan and Middlebrook (1995). One problem with this control technique is the exhibition of subharmonic oscillation if the slope of the compensating ramp is inappropriately selected. This phenomenon has been reported in the early 80's (Redl and Novak , 1981). Since then, its prediction has been widely explored (Chan and Tse , 1997; Holland , 1984; Ridley , 1991; Tse , 1994). However, most of the models used to predict this behavior simplify the regulator as a first-order system, hence allowing to derive, using piecewise linear approximations of the waveforms, a simple closed-form expression to predict the subharmonic instability boundary. The analysis of the perturbed control signal unveils that the boundary of subharmonic oscillation in a current-programmed DC-DC regulator is given by (Erickson and Maksimovic , 2001, chap.11), Lee (2014):

$$-\frac{m_2+m_a}{m_1+m_a}=1, \tag{1}$$

which can conveniently be rewritten as follows:

$$-\frac{1}{2}(m_2+m_1)=m_a, \tag{2}$$

where $m_1>0$ and $m_2<0$ are the slopes of the control signal during the charging (ON) and discharging (OFF) phases respectively and $-m_a<0$ is the slope of the ramp compensator. Based on inductor volt-second balance principle in steady-state regime (Erickson and Maksimovic , 2001, chap.2), one has that $Dm_1=-(1-D)m_2$ and the previous equation can also be expressed as follows

$$(m_1-m_2)(D-\frac{1}{2})=m_a. \tag{3}$$

For stability, m_a must be greater than a certain critical value given by the left side of (1) or equivalently (3). Without using a ramp signal ($m_a=0$), the previous conditions simply become $m_1=-m_2$ or equivalently $D=1/2$. Accordingly, it is broadly believed among the power electronics community that constant switching frequency converters under peak CMC without a compensating ramp signal exhibit subharmonic oscillation for duty cycles $D>1/2$. In the case of a closed voltage loop, the above slope-based criterion for stability prediction is inaccurate and if no compensating ramp is used, subharmonic oscillation can take place even for operating duty cycles values below 1/2 (Ridley , 1991). In some other cases, the opposite may occur, *i.e*, the needed ramp slope to stabilize the system could be lower with closed voltage loop closed than with this loop open. In order to detect these peculiarities, accurate models and analysis techniques such as those based on discrete-time models and Floquet theory combined with Filippov method (Giaouris *et al.* , 2008; Siewniak and Grzesik , 2014) must be used. However, it is not easy to get design-oriented expressions for stability prediction from these techniques.

Some results concerning stability conditions for constant switching frequency PWM power converters with CMC, taking into account the interaction of the current and voltage feedback loops have been first derived in (Redl and Novak , 1981)

and later in (Anunciada *et al.* , 1992) where it has been shown that the stability limit as a function of the steady-state duty cycle can be represented by a second order polynomial function. An early discussion on the effect of the output voltage loop on the subharmonic oscillation is in (Daly , 1982) where it has been also reported that the boundary of instability is not always $D = 1/2$.

On the other hand, in (Rodriguez *et al.*, 2012a), the boundary of subharmonic oscillation in buck-type converters under VMC has been obtained in terms of the ripple magnitude of the feedback signal. In particular, the authors proposed a ripple index defined as the ripple amplitude of the control signal scaled by the ramp modulator amplitude. The approach have allowed compressing the different system parameters into a single ripple-based index. It has also been established that subharmonic oscillation will not be exhibited by the system if the proposed index is less than a critical duty-cycle-dependent value. A closed-form expression involving the matrices describing the state-space model of the system has been obtained in (El Aroudi , 2014-a) for the buck converter under VMC and CMC strategies. Under some *practical* conditions the result can also be approximated by polynomial functions and then reformulated in terms of the ripple of the control signal (Rodriguez *et al.*, 2012a; Rodriguez *et al.* , 2012b). In (Fang , 2013), the concept of predicting subharmonic instability using the ripple index reported in (Rodriguez *et al.*, 2012a) has been *criticized* advocating, using a counter example, that the results obtained from such an approach are inaccurate. However, using either a slope-based or a ripple-based criterion will mainly depend upon the shape of control signal waveforms which in turn depends on the converter topology, control mode, Equivalent Series Resistance (ESR) of the capacitor, and the type of the compensator used. More precisely we will show in this paper that the *relative degree* of the total loop of the system is decisive in determining wether slope or ripple information in the feedback control signal is dominant in the critical stability condition. Namely, for VMC or average current mode control (ACMC) the control signal that is compared to the periodic sawtooth ramp signal can be considered parabolic and the results can be *interpreted* in terms of a ripple index (Rodriguez *et al.*, 2012a). The use of peak/valley CMC or the presence of an ESR such as in the ripple-based V^2 control makes the control signal to contain both ripple information (quadratic terms of the duty cycle) and slope component (first order terms of the duty cycle) (El Aroudi , 2014-a; Rodriguez *et al.* , 2012b). Depending on the values of the ESR of the capacitor and the ratio between feedback coefficients, either the ripple or the slope may be dominant in predicting subharmonic oscillation (El Aroudi , 2014-a) while it is always generally possible to pass from one criterion to another. In some cases a general purpose criterion is needed because nor the simplified expression in (1) nor the ripple-based criterion in (Rodriguez *et al.*, 2012a) are accurate due to the presence of both linear terms (slope) and quadratic terms (ripple) and even higher order terms of the control signal.

In this paper, first a new and simple exact expression for predicting subharmonic instability is presented and then approximated and interpreted in terms of the converter feedback signal slope or ripple depending on the type of the control mode and the converter topology. Based on the work by the authors for VMC (Rodriguez *et al.*, 2012a) and initial work for CMC that was presented in (Rodriguez *et al.* , 2012b), we thoroughly demonstrate the previous claims and we fully explain the originally reported results while extending them to other converters under some practical conditions. Design-oriented expressions are derived for predicting subharmonic oscillation boundary in switching converters under CMC investigating under

what condition, a slope-based and/or a ripple-based index should be used. The approach is applied to different examples of converter topologies and control strategies such as PI and PID compensators. The effect of some relevant parasitic parameters such as the ESR of the output capacitance on the subharmonic oscillation boundary is also revealed.

The rest of the paper is organized as follows. Section II briefly presents the system modeling, the steady-state response and closed-form expressions for two-loop feedback switching regulators. A generalized approximate slope-based expression is derived in the same section, valid for the case of a control signal that can be accurately approximated by straight lines for each switch state. The accuracy of derived expression is checked by numerical simulation using an example of a boost converter. Subsequently, Section III presents a general purpose ripple-based stability criterion for those converters for which switching does not change the state matrix and only the input vector is altered. The accuracy of the simple design-oriented derived expression is demonstrated through different examples of switching converters. In Section IV, the effect of dynamic compensators of the voltage loop on the subharmonic instability boundary of switching regulators under CMC are characterized. The effect of the ESR of the capacitor is addressed in Section V. The role of the ramp compensator on the stability boundary together with some practical recommendations are discussed in Section VI. Limitations of the slope-based and ripple-based index approaches are addressed in Section VII. Finally, some conclusions are given in the last section.

2. Switched Model, Steady-State Response and Subharmonic Oscillation Boundary

Let $v_{\text{ramp}}(t)$ be the $T-$periodic ramp signal used for modulation, compensation or stabilization. The steady-state duty cycle is imposed by the following constraint

$$v_{\text{ramp}}(DT) - v_{\text{con}}(DT) = 0, \tag{4}$$

where $v_{\text{con}} = R_s(i_{\text{ref}} - i_L)$ and R_s is the gain of the current sensor. Generally, the current reference i_{ref} is given by a suitable dynamic controller regulating the output voltage. Extra state variables associated to this controller will be included in the modeling. Taking into account these state variables, the control signal can be written as $v_{\text{con}} = \mathbf{C}(\mathbf{X}_r - \mathbf{x})$, where $\mathbf{X}_r$ is a reference vector whose elements depend on the control mode used, $\mathbf{C}$ is an appropriate vector of feedback coefficients and $\mathbf{x} \in \mathbb{R}^N$ is the vector of the state variables including the power stage and the controller, N being the order of the system. If no external ramp is used, the system switches whenever $v_{\text{con}} = 0$ and the steady-state duty cycle is imposed by this condition. In Continuous Conduction Mode (CCM), the system can be described by:

$$\dot{\mathbf{x}} = \mathbf{m}_1(\mathbf{x}) = \mathbf{A}_1\mathbf{x} + \mathbf{B}_1\mathbf{w} \quad \text{for S ON}, \tag{5a}$$

$$\dot{\mathbf{x}} = \mathbf{m}_2(\mathbf{x}) = \mathbf{A}_2\mathbf{x} + \mathbf{B}_2\mathbf{w} \quad \text{for S OFF}. \tag{5b}$$

$\mathbf{A}_i \in \mathbb{R}^{n\times n}$ and $\mathbf{B}_i \in \mathbb{R}^{n\times w}$, $i = 1, 2$ are the system matrices for phase i and $\mathbf{w} \in \mathbb{R}^w$ is the vector whose elements are the external parameters of the system, w is the number of these parameters. The converter is forced to switch to the first configuration each clock period T and switches to the OFF phase a time $nT + t_s$,

$n \in \mathbb{N}$, whenever the ramp signal crosses the control signal *i.e,* whenever $\mathbf{C}(\mathbf{X}_r - \mathbf{x}) - v_{\text{ramp}} = 0$ at a certain instant t_s. The ratio t_s/T is the duty cycle D for Trailing Edge Modulation (TEM) strategies on which we will focus our study. The results can be adapted for all LEM strategies by just a change of variable $D \rightarrow 1-D$ and a simple sign inversion in the feedback coefficients. Let us define $\mathbf{\Phi}_1 = e^{\mathbf{A}_1 DT}$, $\mathbf{\Phi}_2 = e^{\mathbf{A}_2(1-D)T}$, $\mathbf{\Psi}_1 = \int_0^{DT} e^{\mathbf{A}_1 t} \mathrm{d}t \mathbf{B}_1 \mathbf{w}$ and $\mathbf{\Psi}_2 = \int_0^{(1-D)T} e^{\mathbf{A}_2 t} \mathrm{d}t \mathbf{B_2 w}$. Let $\overline{\mathbf{\Phi}} = \mathbf{\Phi}_2 \mathbf{\Phi}_1$ and let $\overline{\mathbf{\Psi}} = \mathbf{\Phi}_2 \mathbf{\Psi}_1 + \mathbf{\Psi}_2$. Let $\mathbf{x}_0$ be the steady-state value of the $T-$periodic orbit of the system at the beginning of the switching period. If $(\mathbf{I} - \overline{\mathbf{\Phi}})$ is non singular, $\mathbf{x}_0$ can be expressed as follows (El Aroudi , 2014-b):

$$\mathbf{x}_0 = (\mathbf{I} - \overline{\mathbf{\Phi}})^{-1} \overline{\mathbf{\Psi}}. \tag{6}$$

If the matrix $(\mathbf{I} - \overline{\mathbf{\Phi}})$ is singular, the previous expression applies only to the invertible block while the component of the remaining state variables can be obtained separately. A time-domain steady-state analysis of the system $2T-$periodic orbit reveals that, at the boundary of subharmonic oscillation, the following equality holds [1]:

$$m_a = -\mathbf{C}[(\mathbf{I} - \mathbf{\Phi}^2)^{-1} \mathbf{\Phi}_1 (\mathbf{I} - \overline{\mathbf{\Phi}})(\mathbf{m}_1(\mathbf{x}(0)) + \mathbf{m}_2(\mathbf{x}(0)))] \tag{7}$$

where $\mathbf{\Phi} = \mathbf{\Phi}_1 \mathbf{\Phi}_2$. For more details on deriving (7) the readers can see (El Aroudi , 2014-b) where that expression has been derived without using any approximation and without giving design-oriented slope-based or ripple-basesd design expressions. Because $(\mathbf{I} - \mathbf{\Phi}^2)^{-1} = (\mathbf{I} + \mathbf{\Phi})^{-1} (\mathbf{I} - \mathbf{\Phi})^{-1}$ and $\mathbf{\Phi}_1 (\mathbf{I} - \overline{\mathbf{\Phi}}) = (\mathbf{I} - \mathbf{\Phi}) \mathbf{\Phi}_1$, (7) can still be simplified as follows:

$$m_a = -\mathbf{C}(\mathbf{I} + \mathbf{\Phi})^{-1} \mathbf{\Phi}_1 (\mathbf{m}_1(\mathbf{x}_0) + \mathbf{m}_2(\mathbf{x}_0)). \tag{8}$$

The design of switching converters using the previous expression would require a comprehensive knowledge about suitable ways of approximating such expression and finally to get some design guidelines to predict subharmonic oscillation instabilities and to determine either a slope-based or a ripple-based condition can be used for this purpose. This paper, being a continuation of the authors work in (Rodriguez *et al.* , 2012b), takes a step further in achieving these objectives. It should be noted that apart from (El Aroudi , 2014-b; El Aroudi *et al.* , 2015-a), the critical boundary condition as it appears in (8) has never been reported to the authors knowledge. Yet, equivalent expressions expressed differently and obtained from a completely different approach than the one in (El Aroudi , 2014-b; El Aroudi *et al.* , 2015-a) appear in (Fang , 2014). It should also be noted that another kind of instability known as saddle-node bifurcation can also be detected using (8) by just changing $\mathbf{m}_1(\mathbf{x}_0) + \mathbf{m}_2(\mathbf{x}_0)$ by $\mathbf{m}_1(\mathbf{x}_0) - \mathbf{m}_2(\mathbf{x}_0)$ and $\mathbf{I} + \mathbf{\Phi}$ by $\mathbf{I} - \mathbf{\Phi}$ (See (El Aroudi , 2014-b) for derivation details). Another point that is worth to mention here is that although all the study of this paper is based on (8), its objective is not to present or to demonstrate this expression which, together with other details such as the effect of the integral action, is a subject of a further study to be reported later in a separate paper.

[1] Eq. 7 is adapted using the notation of this paper.

In the critical condition given in (2) only the inductor current is considered as a state variable while assuming that the waveforms of this current can be approximated by straight lines for each switch state and that the capacitor voltage and other state variables are constant or very slowly varying. In some converter topologies like the boost converter the straight line approximation can also be applied to the capacitor voltage when the switching frequency is much higher than the natural frequencies of filtering components. Taking this into account, the matrix exponentials in (8) can be approximated by first order terms in their Taylor expansion and accordingly one has that:

$$\begin{aligned}(\mathbf{I}+\mathbf{\Phi})^{-1}\mathbf{\Phi}_1 &\approx (\mathbf{I}+(\mathbf{I}+\mathbf{A}_1DT)(\mathbf{I}+\mathbf{A}_2\overline{D}T))^{-1}(\mathbf{I}+\mathbf{A}_1DT)\\ &\approx (2\mathbf{I}+\mathbf{A}_1DT+\mathbf{A}_2\overline{D}T)^{-1}(\mathbf{I}+\mathbf{A}_1DT)\\ &\approx (2(\mathbf{I}+\frac{1}{2}\mathbf{A}_1DT+\frac{1}{2}\mathbf{A}_2\overline{D}T))^{-1}(\mathbf{I}+\mathbf{A}_1DT)\\ &\approx (\frac{1}{2}(\mathbf{I}-\frac{1}{2}\mathbf{A}_1DT-\frac{1}{2}\mathbf{A}_2\overline{D}T))(\mathbf{I}+\mathbf{A}_1DT)\\ &\approx \frac{1}{2}(\mathbf{I}+\frac{1}{2}\mathbf{A}_1DT-\frac{1}{2}\mathbf{A}_2\overline{D}T). \end{aligned} \tag{9}$$

The accuracy of the approximation is mainly dependent on the spectral radii $sr(\mathbf{A}_1DT)$ and $sr(\mathbf{A}_2\overline{D}T)$ of the matrices $\mathbf{A}_1DT$ and $\mathbf{A}_2\overline{D}T$. The spectral radius of a linear operator $\mathbf{L}$ is the absolute value of the largest eigenvalue of $\mathbf{L}$, *i.e.,*

$$sr(\mathbf{L}) = \sup(|\lambda| : \lambda \in \sigma(\mathbf{L})|). \tag{10}$$

where $\sigma(\mathbf{L})$ is the spectrum of the operator $\mathbf{L}$. If $sr(\mathbf{A}_1DT)$ and $sr(\mathbf{A}_2\overline{D}T)$ are sufficiently smaller than 1, the first terms in (9) are enough for a sufficiently accurate prediction of subharmonic oscillation. If the straight line approximation is valid, (9) can be used in (8) which then can be approximated by:

$$m_a \approx -\frac{1}{2}\mathbf{C}(\mathbf{I}+\frac{1}{2}(\mathbf{A}_1DT-\mathbf{A}_2\overline{D}T))(\mathbf{m}_1(\mathbf{x}_0)+\mathbf{m}_2(\mathbf{x}_0)). \tag{11}$$

If $sr(\mathbf{A}_1DT)\to 0$ and $sr(\mathbf{A}_2\overline{D}T)\to 0$, $\mathbf{A}_1DT$ and $\mathbf{A}_2\overline{D}T$ can be neglected in (11) which then can still be simplified as follows:

$$m_a \approx -\frac{1}{2}\mathbf{C}(\mathbf{m}_1(\mathbf{x}_0)+\mathbf{m}_2(\mathbf{x}_0)). \tag{12}$$

Example 1: Consider the voltage-fed boost converter with a resistive load R and the following values of parameters (Lee , 2014): $R = 6\ \Omega$, $L = 20\ \mu$H, $C = 480\ \mu$F, $v_g = 5$ V, $R_s = 1\ \Omega$. Fig. 1 shows the schematic circuit diagram of the system. Let us neglect the ESR of the capacitor. Note that in this case the output voltage v_o coincides with the capacitor voltage v_C. Consider that the system is under CMC with a programmed peak current value i_{ref} and a simple proportional voltage controller. If the voltage loop is open, i_{ref} is given without external feedback. The duty cycle D can be varied by modifying this current reference. If the voltage loop is closed, i_{ref} will be programmed by the outer voltage loop and the duty cycle D can be varied by adjusting the voltage reference v_{ref} of the voltage loop. Let the

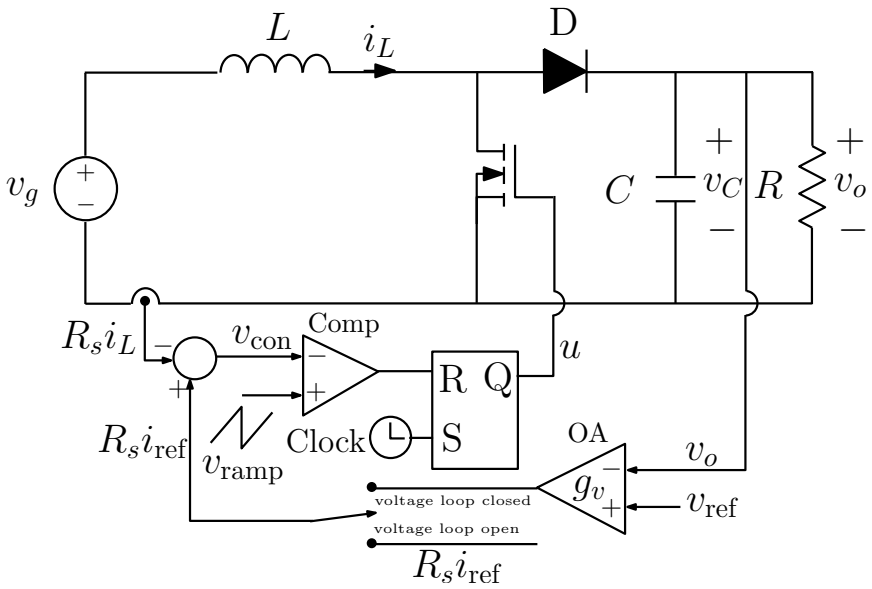

Figure 1. Schematic circuit diagram of the boost converter of Example 1.

state vector be $\mathbf{x} = (v_C, \ i_L)^\intercal$. Fig. 2 shows the plot of the minimum required ramp slope m_a (normalized to $v_g R_s/L$) for avoiding subharmonic oscillation as a function of the operating steady-state duty cycle D with both open and closed voltage loop. Both exact and different approximate curves are plotted for two different values of the voltage feedback gain g_v. The stable region is the one that is above the boundary curves. The result in this example is an indication that the straight line approximation is valid for practical purposes with voltage loop open and closed. It is in these cases that the slope based approximations in (11) and (12) are sufficiently accurate while (2) could still lead to inaccurate results with voltage loop closed. Two interesting conclusions can be drawn from the results shown in Fig. 2.

- A compensating ramp could be needed even for $D < 1/2$ if the outer voltage loop is closed.
- For $D > 1/2$, the needed slope m_a is smaller with voltage loop closed than with open voltage loop. For this particular case, the voltage loop improve the stability at the fast scale.

One can observe that with voltage loop closed, the subharmonic oscillation area is reduced. This happens because of the contribution of the voltage loop in the process of ramp compensation. The voltage feedback contributes with a slope in addition to the inductor current slope, and this works in exactly the same way as the compensating ramp. The amount of slope contributed by the voltage feedback can be deduced from (11). In most topologies like the boost converter for which the output voltage can be approximated by pieces of straight lines, the amount of slopes contributed by the output voltage feedback will help in stabilizing the system for a certain range of the duty cycle larger than 1/2. Time domain simulation from a circuit-level switched model implemented in PSIM© software has been used to validate the theoretical predictions.

The waveforms of the state variables and the control signals without ramp compensation ($m_a = 0$, in which P_1 lies) shows that a stable $T-$perioric behavior is obtained for a duty cycle $D = 0.48$ with open voltage loop. With the same value of

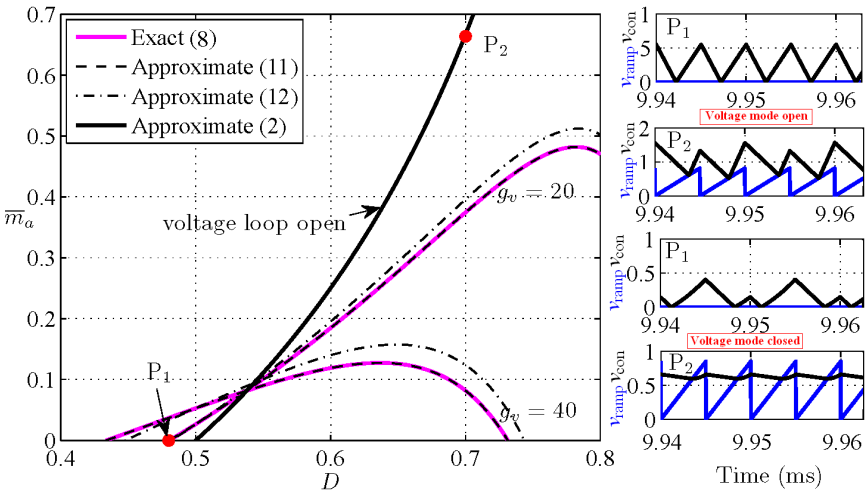

Figure 2. Stability curves of the boost converter of Example 1 in the plane $(D, \overline{m}_a)$. Time-domain waveforms corresponding to points P_1 with $D = 0.48$ and P_2 with $D = 0.7$ are shown considering closed voltage loop with $g_v = 40$ and $g_v = 20$ respectively and considering open voltage loop. For this example, the curves corresponding to the exact expression (8) and the approximated expression (11) are almost coincident.

duty cycle but with closed voltage loop, the system exhibits subharmonic oscillation. For $D = 0.48$, no ramp compensator is needed with the voltage loop open while a compensating ramp with a minimal normalized slope $\overline{m}_a = 0.0369$ is required when the loop is closed with $g_v = 40$. For $D > 1/2$, it may occur the opposite and the minimum needed slope m_a could be smaller when the voltage loop is closed. According to Fig.2, for $D = 0.7$, the needed ramp slope for stabilization with voltage loop open is $\overline{m}_a = 0.668$ while it is smaller ($\overline{m}_a = 0.37$) when the loop is closed with $g_v = 20$ or ($\overline{m}_a = 0.0818$) with $g_v = 40$.

Eqs. (11) and (12) have extended the slope-based criterion for predicting subharmonic instability boundary to switching regulators under CMC with voltage loop closed, hence demonstrating that the stability boundary has a dependency on the amount of the slope added by the voltage-feedback loop in addition to the inductor slopes. The subharmonic oscillation boundary condition expressed in (11) and (12) can be applied to CMC with voltage loop open or closed. Moreover, the expression reveals the effect of some converter parameters, not appearing in (1), on the stability boundary. This is the case, for example, of the gain g_v of the voltage loop and the capacitance C of the output capacitor.

Remark 1: *The approximation in* (9) *is equivalent to considering only the first two terms in the Taylor series expansion of the matrix exponential. It is not surprising that keeping only these terms gives an accurate result because the time constant of the filtering components are much larger than the switching period, and because the state variables (both voltage and current) are practically straight lines for each switch state as can be observed from the waveforms in Fig. 2. However, this is not always the case. In particular, when* $\mathbf{A}_1 = \mathbf{A}_2 := \mathbf{A}$*, the straight line approximation is no more valid for all the variables. Although the inductor current waveforms can be approximated by first order terms of the matrix exponential components, second order terms are needed for an accurate approximation of the capacitor voltage.*

Remark 2: *When* $\mathbf{A}_1 = \mathbf{A}_2 := \mathbf{A}$*, the steady-state value* $\mathbf{x}_0$ *given in* (6) *can be approximated by the following expression:*

$$\mathbf{x}_0 \approx -\mathbf{A}^{-1}(\mathbf{B}D + \mathbf{B}_2\mathbf{w}), \tag{13}$$

where $\mathbf{B} = (\mathbf{B}_1 - \mathbf{B}_2)\mathbf{w}$. *Using* (12) *leads to*

$$m_a \approx \mathbf{CB}(D - \frac{1}{2}). \tag{14}$$

Under CMC with open voltage loop, (14) *is accurate enough because the component corresponding to output voltage feedback in the vector* $\mathbf{C}$ *is zero, making also null the second order term. With closed voltage loop, second order terms are non zero and are necessary for an accurate prediction of the stability boundary.*

Example 2: Consider a buck converter under CMC with voltage loop closed by a PI controller with proportional gain g_v and time constant τ_i. Let us consider the following values of parameters which are oriented to miniaturization (Rodriguez *et al.*, 2012a): input voltage v_g=6 V, output voltage reference V_{ref}=3.6 V, laod resistance R=2.5 Ω, inductance of the inductor L=66 nH, capacitance of the output capacitor C=20 nF, sensor current gain $R_s = 1$ Ω, switching frequency $f_s = 1/T$=50 MHz and time constant of the integrator τ_i =0.1 μs. Let the state vector be $\mathbf{x} = (v_C,\ i_L,\ e_v)^\intercal$, where e_v is the integral of the output voltage error. Fig. 3 shows the schematic circuit diagram of the system and Fig. 4 shows its stability map with the voltage loop open and closed for different values of the feedback voltage gain g_v. Using (14), one would predict that no ramp compensator is needed for a buck converter under a purely VMC!. This is not correct and in fact the ramp slope needed in VMC is always larger than in the case of CMC as can be clearly observed in the Fig. 4. Since the approximate expression (14) does not depend on the feedback gain g_v, the approximate curve from this expression coincides with the curve corresponding to a pure CMC with voltage loop open. However, the exact stability curves show that the voltage loop modifies the boundary of subharmonic oscillation and that by increasing the value of the voltage gain g_v, the stability area is reduced. This also occurs if the capacitance C is decreased. Note also that, as the voltage feedback gain is increased, the reduction of the stability region is accompanied by an increase of the curvature of the time domain waveforms of the control signal as well as the boundary lines in terms of the operating duty cycle because of the increasing influence of quadratic terms missing in (1)-(3) and (14).

3. From a slope-based to a ripple-based criterion

In compact form, the switched model given in (5a)-(5b) can be expressed as follows:

$$\dot{\mathbf{x}} = \mathbf{m}_2(\mathbf{x}) + \underbrace{(\mathbf{m}_1(\mathbf{x}) - \mathbf{m}_2(\mathbf{x}))}_{\mathbf{B}} u(t). \tag{15}$$

In the buck converter, the term $\mathbf{m}_1(\mathbf{x}) - \mathbf{m}_2(\mathbf{x})$, denoted as $\mathbf{B}$, does not depend on the state variables because $\mathbf{A}_1 = \mathbf{A}_2$. In most converter topologies, this term depends only on the capacitor voltage as a state variable which can be considered practically constant during a switching cycle. Therefore $\mathbf{B}$ can also be considered independent on the state variable $\mathbf{x}$. Although strictly speaking this is the case of the simple buck converter with ideal switching devices for which $\mathbf{A}_1 = \mathbf{A}_2$, it is also the case of most switching converters feeding a constant voltage load such as a battery (Kabe *et al.* , 2007) or connected to a dc link voltage in grid connected inverters. Note also that even in the buck converter, if parasitic resistances in the input voltage

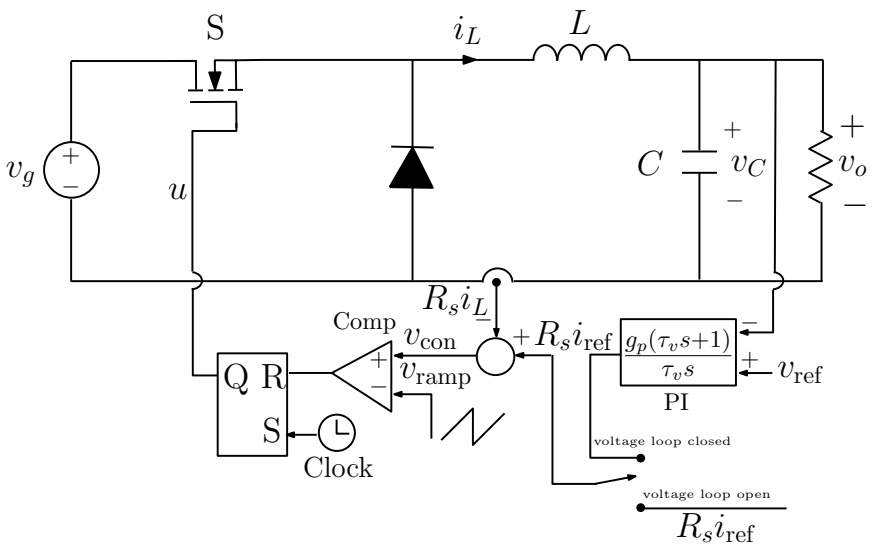

Figure 3. Schematic circuit diagram of the buck converter of Example 2.

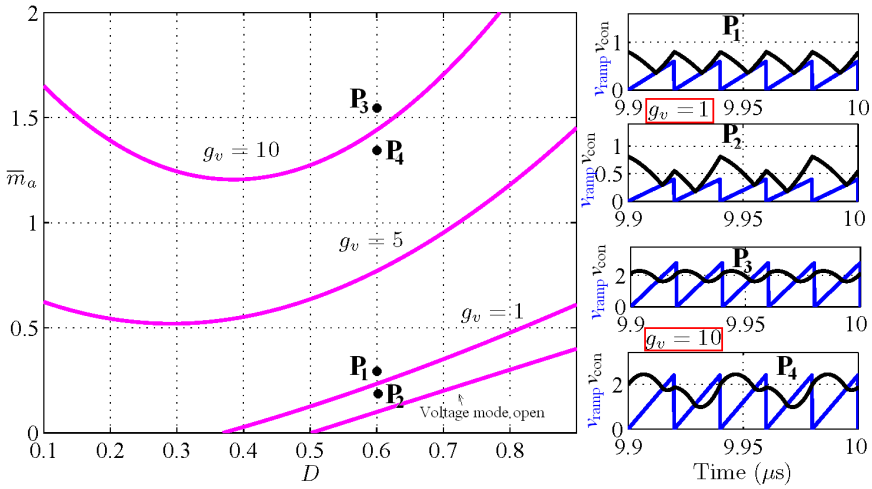

Figure 4. Stability boundaries from (8) in the plane $(D, \overline{m}_a)$ for the buck converter of Example 2 for different values of g_v. The stable regions are above the curves.

source or in the switching devices are taken into account, the corresponding state matrices $\mathbf{A}_1$ and $\mathbf{A}_2$ will be different (Tsai and Chen , 2014). However, since these parasitics are small in practice, the results that would be obtained by using $\mathbf{A}_1 = \mathbf{A}_2$ will be enough accurate. Under all these conditions, the dynamical behavior of the system can be approximately represented by the following state-space model:

$$\dot{\mathbf{x}} = \mathbf{A}\mathbf{x} + \mathbf{B}u + \mathbf{B}_2\mathbf{w}, , \tag{16a}$$

$$v_{\text{con}} = \mathbf{C}(\mathbf{X}_r - \mathbf{x}). \tag{16b}$$

One can note that the u-to-v_{con} loop is linear and therefore some techniques and concepts from linear system theory can be applied without averaging the system switched model. It has been shown in (El Aroudi *et al.* , 2015) that by expanding (8) as a Taylor series, the subharmonic instability boundary can be described by

the following equality:

$$\begin{aligned} m_a &= \sum_{k=1}^{\infty} \mu_{k-1} \mathcal{S}_k(D) T^{k-1} \\ &= \mu_0 (D - \frac{1}{2}) + \mu_1 T (\frac{D^2}{2} - \frac{D}{2} + \frac{1}{4}) \\ &+ \mu_2 T^2 (\frac{D^3}{6} - \frac{D^2}{4} + \frac{D}{12}) \\ &+ \mu_3 T^3 (\frac{D^4}{24} - \frac{D^3}{12} + \frac{D^2}{24} - \frac{1}{48}) + \dots \end{aligned} \tag{17}$$

where $\mu_k = \mathbf{C}\mathbf{A}^{k-1}\mathbf{B}, k = 1, 2....$ are known as the Markov parameters of the system described by the realization $(\mathbf{A}, \mathbf{B}, \mathbf{C}, \mathbf{0})$ (Corriou , 2004) and $\mathcal{S}_k(D)$ are special functions that can be expressed in terms of scalar Clausen polynomial functions (Lewin , 1981). Usually, the terms $\mu_k T^k$ for $k \geq 2$ are negligible because in most applications of switching regulators, the switching frequency is much higher than the natural frequencies of the power stage circuit and filtering components and therefore, in such cases, the first two terms $\mu_0 \mathcal{S}_1$ and $\mu_1 T \mathcal{S}_2$ are sufficient to predict subharmonic oscillation. It can be observed that the presence of these terms depends mainly on the value of the relative degree of the u-to-v_{con} loop. In switching converters under peak/valley CMC *with voltage loop open, or under ripple-based V^2 control,* the relative degree is 1 and only the first order term $\mu_0(D - 1/2)$, which is related to the slopes of the control signal, is dominant in predicting subharmonic instability. Higher order terms are just corrective terms. In all those converters with relative degree higher than 1, the first order term $\mu_0(D - 1/2)$ is not present in the expression of the stability border because $\mu_0 = 0$, and therefore it is necessary to use high order terms. This is the case for instance of VMC in buck converters. If the spectral radius $sr(\mathbf{A}T)$ of the matrix $\mathbf{A}T$ is sufficiently smaller than 1, only the second term, mainly related to the ripple of the control signal, will be dominant. If the relative degree is equal to 1 with voltage loop closed, which is the case of most practical converters, both first order (linear) $\mu_0(D - 1/2)$ and second order (quadratic) terms $\mu_1(1 - 2D\overline{D})$ are present while high order terms are negligible if $sr(\mathbf{A}T) \ll 1$. Ignoring terms for $k \geq 3$, the boundary condition in (17) becomes as follows

$$\mu_0 (D - \frac{1}{2}) + \mu_1 \frac{1}{4} (1 - 2D\overline{D}) T \approx m_a. \tag{18}$$

The previous expression in (18) can be particularized for different control schemes and switching regulators. It shows that, generally, the conditions for subharmonic oscillation occurrence in VMC and CMC are apparently very similar. The main issue to distinguish between them is to know which term is dominant in this expression. In order to show that (18) can also be interpreted in terms of the ripple amplitude of the control signal instead of its slope, let us divide the expression by m_a ($m_a = V_M/T = V_M f_s$), and multiply it by $D\overline{D}$ hence obtaining:

$$\mu_1 \frac{D\overline{D}}{8 V_M f_s^2} \approx (1 - \frac{\mu_0}{m_a}(D - \frac{1}{2})) \frac{D\overline{D}}{(2 - 4D\overline{D})}. \tag{19}$$

We will see through some examples that the left hand side of (19) when μ_1 is specified is nothing but the ripple of the control signal relative to that of the ramp compensator signal.

Example 3: Take Example 2 and let the state vector be $\mathbf{x} = (v_C,\ i_L\ , e_v)$, where e_v is the integral of the output voltage error. The terms $\mu_{k-1}T^{k-1}$, for $k = 1, 2$, are

$$\mu_0 = \mathbf{CB} = R_s\frac{v_g}{L},\ \ \mu_1 T = \mathbf{CAB}T = g_v\frac{v_g}{LC}T. \tag{20}$$

Because $T^2/(LC) \ll 1$ in all practical converters, only the first two terms are needed and (19) can be expressed as follows:

$$\frac{g_v}{V_M}\frac{v_g D\overline{D}}{8LCf_s^2} \approx (1 - \frac{R_s}{m_a}\frac{v_g}{L}(D - \frac{1}{2}))\frac{D\overline{D}}{(2 - 4D\overline{D})}. \tag{21}$$

Although, many different approximate expressions for the ripple amplitude Δv exist (Singh , 2014), the following simple but widely used expression is considered (Erickson and Maksimovic , 2001, chap.2):

$$\Delta v = \frac{v_g D\overline{D}}{8LCf_s^2} \tag{22}$$

Therefore, the left side of (21) is clearly related to the ripple of the output voltage and hence this equation can be written as follows:

$$\rho_v = \rho_{\text{cr,CMC}}, \tag{23}$$

where ρ_v is the ripple-based index defined by:

$$\rho_v = \frac{g_v}{V_M}\Delta v. \tag{24}$$

Its critical value $\rho_{\text{cr,CMC}}$ for subharmonic oscillation occurrence under CMC is given by:

$$\rho_{\text{cr,CMC}} = (1 - \frac{R_s}{m_a}\frac{v_g}{L}(D - \frac{1}{2}))\rho_{\text{cr,VMC}}. \tag{25}$$

and $\rho_{\text{cr,VMC}}$ is the critical value of the ripple obtained in (Rodriguez *et al.*, 2012a) for the VMC case ($R_s = 0$), rewritten here for easy reference

$$\rho_{\text{cr,VMC}} = \frac{D\overline{D}}{2 - 4D\overline{D}}. \tag{26}$$

Eq. (23) has extended the ripple-based index for predicting subharmonic instability boundary to the CMC under the condition that $\mathbf{m}_1 - \mathbf{m}_2$ is independent on the state variables hence demonstrating that the stability boundary has a clear dependency on the amount of the voltage ripple added by the voltage-feedback loop apart from the inductor slopes. Fig. 5 shows the needed ramp slope (normalized to $R_s v_g/L$) for avoiding subharmonic oscillation for different values of g_v. Both the exact curves from (8) and the approximated one based on the ripple-based index from (21) are

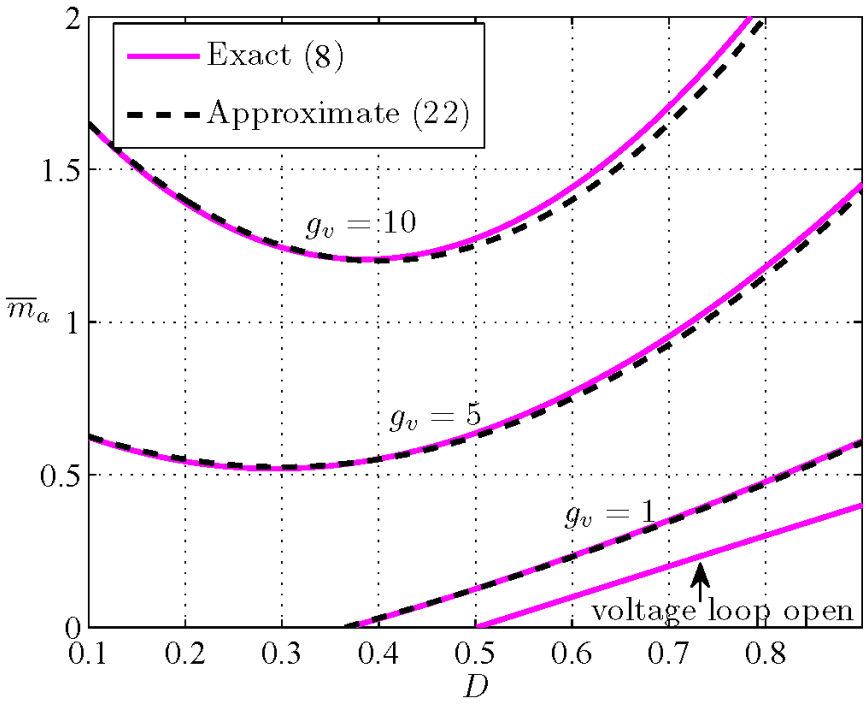

Figure 5. Exact and approximate stability boundaries in the plane $(D, \overline{m}_a)$ for the buck converter of Examples 2 and 3 for different values of g_v .

plotted. For all values of g_v, the exact curve and the one based on the ripple index are almost coincident demonstrating that the design-oriented ripple-based approach can be used without losing accuracy in predicting the onset of instability.

The expressions given in (21) or (23) apply to both VMC and CMC. Parameters such as the feedback gain g_v or the capacitance C, whose effect on modifying the voltage ripple of the control signal is evident explicitly appear in the previous equations and therefore if the variation of these parameters makes the control signal ripple to reach the critical value, the system will exhibit subharmonic oscillation. Although it is expressed in terms of a ripple index that compresses all the parameters of the system, (21) can be solved for any system parameter. For instance, according to this equation, the minimum capacitance guaranteeing stability is given by:

$$C_{\min} = \frac{g_v v_g (1 - 2D\overline{D})}{2f_s(2m_a L + (1-2D)R_s v_g)}. \tag{27}$$

This minimum capacitance can be particularized for pure VMC by letting $R_s = 0$ or for a converter without ramp compensation making $m_a = 0$. In the last case, (21) becomes as follows:

$$\rho_{v,0} = \rho_{\mathrm{cr,CMC,0}}, \tag{28}$$

where $\rho_{v,0}$ and $\rho_{\mathrm{cr,CMC,0}}$ are given by

$$\rho_{v,0} = g_v \Delta v, \ \rho_{\mathrm{cr,CMC,0}} = -\frac{R_s v_g}{f_s L}(D - \frac{1}{2})\frac{D\overline{D}}{(2 - 4D\overline{D})}. \tag{29}$$

In this case, the value of the inductance will not have any effect on the boundary because it appears in both sides of the equality with the same proportion. This is also the case of the input voltage v_g. The switching frequency has more effect on the ripple amplitude than on the slope, and it can be noticed that decreasing its value could lead to the exhibition of subharmonic oscillation.

Example 4: Consider the current-fed boost converter with a constant voltage

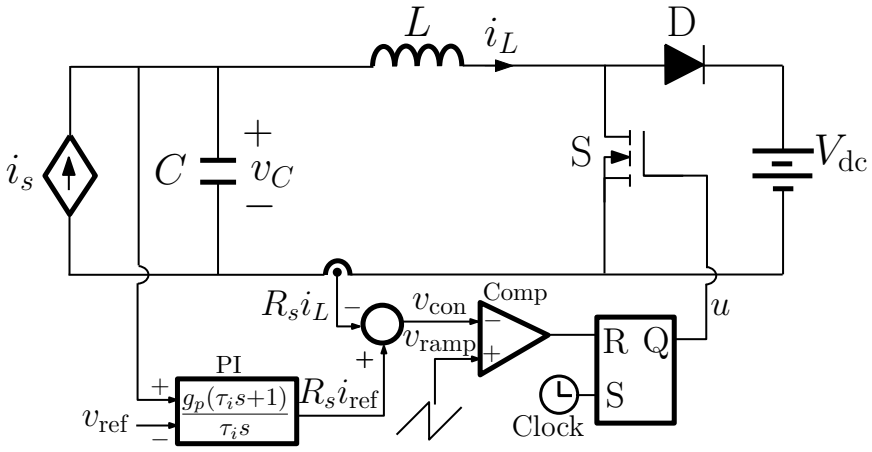

Figure 6. A current-fed boost converter under CMC with input voltage feedback for PV applications.

as a load for photovoltaic (PV) applications (Bianconi *et al.* , 2012). The input current source I_s represents the model of a PV panel and the constant voltage can represent a storage battery or a dc bus. As the solar irradiation or the temperature change during the operation, the voltage of the PV array is adjusted to correspond to the maximum available power. The PV array operating point can be adjusted by regulating the voltage and/or current at the terminals of the array. The input capacitor voltage of the system is controlled using a PI controller to track a reference which is usually dictated by an MPPT controller making the system to operate at the maximum power of the PV array regardless of the weather conditions. Fig. 6 shows the circuit diagram of the system under CMC with input voltage feedback. Let the state vector be $\mathbf{x} = (v_C,\, i_L\,, e_v)$, where e_v is the input voltage error integral. The terms $\mu_{k-1}T^{k-1}$ for this system are:

$$\mu_0 = \mathbf{CB} = R_s\frac{V_{\rm dc}}{L},\;\; \mu_1 T = \mathbf{CAB}T = g_v\frac{V_{\rm dc}T}{LC}. \tag{30}$$

Stability boundaries similar to the one obtained for the previous examples can be obtained for this system. In particular, without ramp compensation ($m_a = 0$) and from (29), the minimum capacitance for avoiding instability is

$$C_{\rm min,1} = \frac{g_v T}{2R_s}\frac{1-2D\overline{D}}{1-2D}, \tag{31}$$

implying that the converter will be unstable for $D > 1/2$ because no positive capacitance can be obtained as a solution of (31) while it will be stable if the capacitance is selected larger than $C_{\rm min,1}$ for $D < 1/2$. Note however that very close to $D = 1/2$, a huge value of capacitance is needed for stability. It is worth also noting that no dependence of the capacitance appears in the slope-based condition (1) and that

the minimum capacitance for a relative ripple less than 1% as required in practical converters is given by;

$$\frac{\Delta v}{DV_{\rm dc}} = 1\% \Rightarrow C_{\rm min,2} = \frac{100\overline{D}}{8Lf_s^2}. \tag{32}$$

It may happen that $C_{\rm min,1} > C_{\rm min,2}$ which implies that even if the output voltage ripple constraint (32) is fulfilled, subharmonic oscillation may still occur.

4. Effect of voltage loop compensators

Many dynamic compensators can be used for controlling switching converters depending on the required performances of the system. These performances depend on the relative degree total loop of the system. A relative degree equal to 1 is required in most applications. All those controllers can be classified into the category of PID compensators (Erickson and Maksimovic , 2001, chap.9), (Kapat 2012 and Krein , 2012). The integrative term in a PID controller is added to get a zero steady-state error making the gain infinite at zero frequency. The effect of this term on subharmonic instability boundary will be negligible if the time constant of the integrator is much higher than the switching period which is the case in practical converters and the previous examples. Note that the time constant of the PI controller is the inverse of its zero, that is usually placed below the resonance frequency which, in turn, is much smaller than the switching frequency. The derivative term is only used for power stages with relative degree 2 hence speeding up the system response while improving stability margin at the slow scale or low frequency. This term is never needed for power stage with relative degree 1. For instance, the derivative term will not be used for controlling the inductor current of elementary converters because the relative degree of these converters is 1 when the inductor current is considered as the output to be controlled. In general, the compensator is selected in such a way that the total loop of the system can be approximated by a pure integrator near the crossover frequency of the total loop gain of the converter.

4.1. *Case of an ideal PID compensator*

The transfer function of a PID voltage-mode controller is usually selected as follows:

$$G_c(s) = g_p \left(\frac{\tau_d \tau_i s^2 + \tau_i s + 1}{\tau_i s} \right), \tag{33}$$

where τ_d and τ_i are the derivative and the integrative time constants respectively and g_p is a suitable gain. This PID controller introduces one pole in the origin and two zeroes $(\omega_{z1},\, \omega_{z2}) = -1/(2\tau_d) \pm \sqrt{1/(2\tau_d)^2 - 1/(\tau_d\tau_i)}$ which are placed close to the resonant frequency of the converter power stage by appropriately selecting the time constants τ_d and τ_i. The description of the compensator in the time-domain is as follows:

$$v_{\rm con} = g_p \left(v_e + \frac{1}{\tau_i} \int_{-\infty}^{t} v_e {\rm d}\tau + \tau_d \frac{{\rm d}v_e}{{\rm d}t} \right), \tag{34}$$

where $v_e = v_{\rm ref} - v_C$ is the voltage error. In the case of voltage-fed buck converters with a resistive load or with a current sink I_s as a load or current-fed boost converters supplying constant voltage load such as a battery, it is possible to rewrite the control voltage $v_{\rm con}$ as a function of the capacitor voltage v_C and the inductor current i_L, since $\mathrm{d}v_e/\mathrm{d}t$ indeed includes both state variables, hence allowing a similar analysis to that carried out in the precedent section. For these systems, the derivative term can be expressed as follows:

$$\frac{\mathrm{d}v_e}{\mathrm{d}t} = -\frac{\mathrm{d}v_C}{\mathrm{d}t} = -\frac{i_L}{C} + \frac{v_C}{RC}. \tag{35}$$

Thus, the feedback gains g_v and R_s which multiply the state variables v_C and i_L respectively become as follows:

$$g_v \to g_p \left(1 - \frac{\tau_d}{RC}\right), \text{ and } \quad \overline{R}_s \to R_s + \frac{g_p \tau_d}{C}. \tag{36}$$

While it is well known that adding a derivative term to the compensator peed up the system response hence improving the phase margin at the slow-scale dynamics, it can also be deduced from (36) that this term has an strong effect upon fast scale dynamics and subharmonic instability by adding the inductor current to the feedback loop and therefore the stability boundary given in (23) applies in this case even if $R_s = 0$ (VMC).

Example 5: Consider Example 2, remove the current loop and use a PID controller with the transfer function given in (**??**). The controller coefficients have been selected by placing $\omega_{z1} = 1/\sqrt{LC}$; $\omega_{z2} = 0.5/(RC)$. For this example, the terms $\mu_{k-1}T^{k-1}$, for $k = 1, 2$, are given by:

$$\mu_0 = g_p \frac{\tau_d v_g}{LC}, \;\; \mu_1 T = g_p \left(1 - \frac{\tau_d}{RC}\right) \frac{v_g}{LC} T. \tag{37}$$

Fig. 7 shows the stability map of the system in terms of the duty cycle D and the normalized ramp slope $\overline{m}_a = m_a/(v_g/L)$. A remarkable agreement can be observed between the exact curves from (8) and the approximated ones from (18) for all the values of g_p. It can be observed in this example that by increasing the voltage gain, the current gain is also increased and the stability boundaries are similar to pure CMC case even if a pure VMC is used. Note however that the second order term related to the voltage ripple is needed for an accurate prediction, although its weight is not strong enough to change the shape of the stability curve which can be approximated with a straight line as in pure CMC case but the critical value of the duty cycle when $m_a = 0$ is no longer 1/2. According to (18), the new critical value is given by:

$$D_c = \frac{1}{2} - \frac{1}{\mu_1 T}\left(\mu_0 - \frac{1}{2}\sqrt{4\mu_0^2 - \mu_1^2 T^2}\right). \tag{38}$$

The dynamics of the system has been checked by numerical simulations using the switched model and a perfect agreement has been obtained as it can be observed in the time-domain waveforms shown in Fig. 7 for $g_p = 5$.

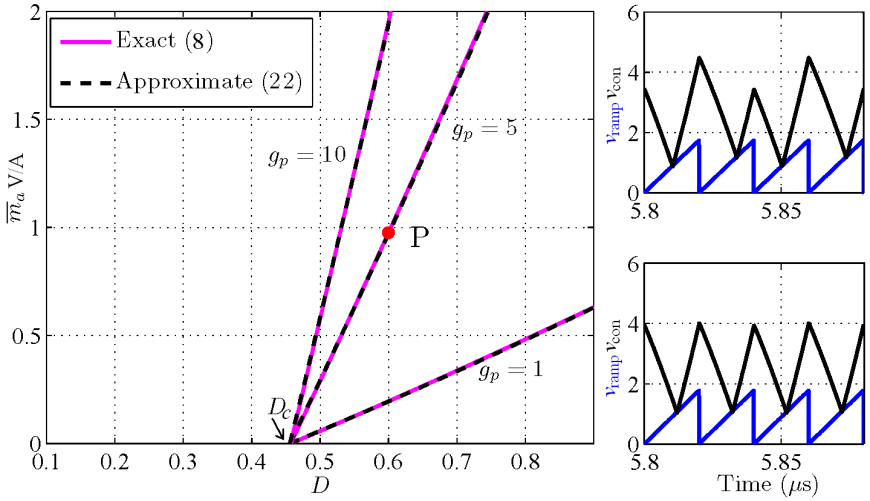

Figure 7. Exact and approximate stability maps of the buck converter of Example 5 and time-domain waveforms of $v_{\rm con}$ and $v_{\rm ramp}$ near point P for $g_p = 5$ just after ($\overline{m}_a = 0.957$ V/A) and just before ($\overline{m}_a = 0.979$ V/A) occurrence of subharmonic oscillation.

4.2. *Case of a realistic PID compensator and type II controller*

The transfer function of a realistic PID is given by the following transfer function with a second pole $\omega_p = 1/\tau_p$:

$$= g_p(\frac{\tau_d\tau_i s^2 + \tau_i s + 1}{\tau_i s(s\tau_p + 1)}). \tag{39}$$

Its description in the time-domain is as follows:

$$\frac{\mathrm{d}e_p}{\mathrm{d}t} = \frac{e_v - e_p}{\tau_p},\ \frac{\mathrm{d}e_v}{\mathrm{d}t} = v_{\rm ref} - v_C, \tag{40}$$

$$v_{\rm con} = g_p\left(\tau_d\frac{\mathrm{d}^2e_p}{\mathrm{d}t^2} + \frac{\mathrm{d}e_p}{\mathrm{d}t} + \frac{e_p}{\tau_i}\right). \tag{41}$$

where e_p and e_v are additional state variables of the system. Therefore, $\mathbf{x} = [v_C,\ i_L,\ e_v,\ e_p]^\intercal$and $\mathbf{C} = [g_p\tau_d/\tau_p,\ R_s,\ -g_p(1/\tau_p - \tau_d/\tau_p^2),\ g_p(1/\tau_p - 1/\tau_i - \tau_d/\tau_p^2)]$. From a design standpoint, it is interesting to know the effect of the pole ω_p. This pole is usually selected in such a way as to reduce the effect of switching noise in the circuit and it is recommended to place it between $f_s/2$ and f_s (Lee , 2014).

Example 6: Consider Example 2, remove the current loop and use a VMC with a PID controller with an additional filter with corner frequency $\omega_p = 1/\tau_p$ (Eq. (39)). Select the controller coefficients by placing $\omega_{z1} = 1/\sqrt{LC}$, $\omega_{z2} = 0.5/(RC)$, $g_p = 5$ and let us vary ω_p. For this example, the terms μ_0 is zero and $\mu_1 T$ and $\mu_2 T^2$ are:

$$\mu_1 T = \frac{g_p\tau_d v_g}{\tau_p LC}T,\ \mu_2 T^2 = g_p\left((\frac{\tau_p - \tau_d}{\tau_p^2}) - \frac{\tau_d}{\tau_p RC}\right)\frac{v_g}{LC}T^2 \tag{42}$$

Fig. 8 shows the stability map illustrating the effect of ω_p on the subharmonic instability boundary which is plotted as a function of the duty cycle D and $\overline{m}_a = m_a/(v_g/L)$. It can be observed that when the second pole ω_p is fixed well below

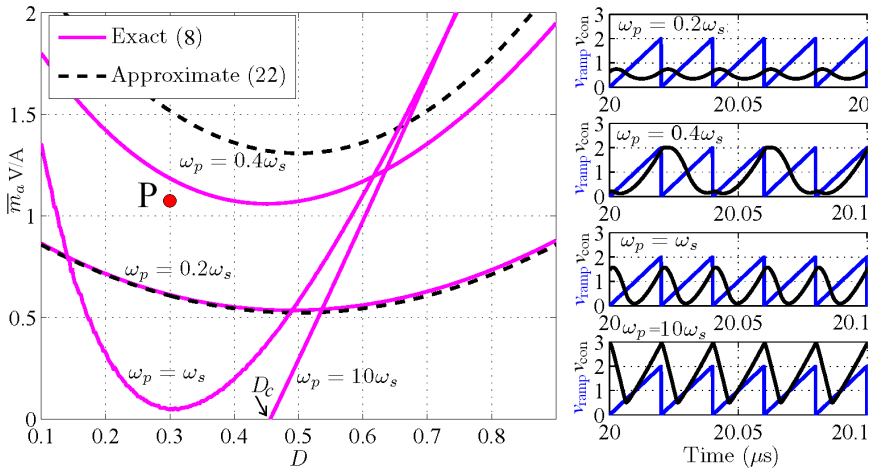

Figure 8. Effect of the second pole ω_p on the exact (8) and approximate (18) stability boundaries of the buck converter of Example 6 and waveforms of the control signals v_{ramp} and v_{con} in point P in the stability map for different values of ω_p.

$\omega_s = 2\pi f_s$, the same stability boundary of a converter under PI controller is obtained with the values of the feedback gains adapted as in (36) hence requiring a ramp compensator for all duty cycles like in Examples 2 and 3. On the opposite, if such a pole is fixed well above the switching frequency, the stability boundary in this case is very similar to the one corresponding to the ideal PID controller in Example 5 and the ramp compensator is needed only for duty cycles larger than the critical value D_c in (38).

Remark 3: *The parameter $\omega_p = 1/\tau_p$ has a significant influence when it is selected near ω_s and therefore the exact expression of the stability boundary* (8) *must be used for an accurate prediction. Fortunately, for $\omega_p \ll \omega_s$ and $\omega_p \gg \omega_s$ the first two terms are sufficient to predict accurately subharmonic oscillation. In the first case, only the term $\mu_1 T$ is needed ($\mu_0 = 0$) and the stability curves can be approximated by parabola similar to pure VMC with PI compensator. In the second case, ω_p has practically no effect and the situation is similar to an ideal PID controller without additional filter and therefore the stability curves corresponding to this compensator apply in this case.*

Remark 4: *Although a pure VMC was considered in Example 6, its results are also valid for the case of a converter under CMC ($R_s \neq 0$) with a voltage loop closed using type II controller ($\tau_d = 0$). The only difference is that one of the zeroes of the system will be imposed by the current feedback and not by the derivative term of the PID controller and therefore only the feedback vector* $\mathbf{C}$ *must be adapted to take into account this difference.*

5. Effects of series resistance of the capacitor

Many parasitic elements can be included in the study. However, from a dynamic point of view only the ESR r_C of the capacitor has a significant effect. The effect this resistance has upon subharmonic instability boundary is taken into account in this section for the case of voltage-fed buck converters and current-fed boost converters, since, indeed, it has an equivalent effect of adding a current feedback to the control.

This is because when $r_C \neq 0$, the output voltage v_o can be expressed as follows:

$$v_o = v_C + r_C i_C = v_C + r_C C \frac{\mathrm{d}v_C}{\mathrm{d}t}, \tag{43}$$

where v_C is the capacitor voltage whose time derivative includes current information. For the case of a resistive load, the voltage v can be expressed as follows:

$$v = \kappa_c (v_C + r_C i_L), \tag{44}$$

where $\kappa_c = R/(R + r_C)$. The state feedback gains become

$$\overline{g}_v \to \kappa_c g_v \qquad \text{and} \qquad \overline{R}_s \to \kappa_c g_v r_C + R_s. \tag{45}$$

One can observe that even if the current loop is open ($R_s = 0$), its effect on the system dynamics will still exist because of the term $\kappa_c g_v r_C \neq 0$. With this parasitic effect, the effective gain of the voltage will be slightly smaller and the feedback gain of the current will be larger. Both effects have a tendency to enlarge the stability region. This will be, for example, the case of ripple-based V^2 control largely based on using the ESR r_C to speed-up the system response without using CMC. The previous effects will not only take place in voltage-fed buck converter with a resistive load and controlled output voltage but also in current-fed boost converter with controlled input voltage v_{in} which can be expressed by:

$$v_{\mathrm{in}} = v_C + r_C (i_L - I_s), \tag{46}$$

Therefore, the state feedback gains become as follows:

$$\overline{g}_v \to g_v \qquad \text{and} \qquad \overline{R}_s \to R_s + g_v r_C. \tag{47}$$

Note that in both cases, when $r_C \neq 0$, an increase in the voltage feedback gain will imply an increase also in the effective current feedback gain and that the results of Example 5 are also valid by making $\tau_d = 0$. In this case the role of the zero introduced by the derivative action will be replaced by the zero $1/(r_C C)$ corresponding to the ESR r_C.

6. Discussion on avoiding subharmonic oscillation and practical recommendations

Subharmonic oscillation is usually avoided by appropriately selecting the slope of the compensating ramp. Most of the design methods for selecting this slope use a first order of the converter ignoring the output voltage loop and its corresponding dynamics. In this section we explain how the stabilizing ramp compensation in current-programmed switching converters is affected by the voltage loop by using the closed-form expression (17) derived in Section V. In order to clearly see the effect of the voltage loop, the critical ramp slope m_a for avoiding subharmonic oscillation according to Eq. (17) is the sum of two terms and can be expressed as follows:

$$M_1(D) + M_2(D) = m_a, \tag{48}$$

where the terms $M_1(D)$, like (3), depends linearly on the steady-state duty cycle and can be expressed as follows:

$$M_1(D) = \mu_0(D - \frac{1}{2}), \tag{49}$$

and M_2 has a more complex form that can be expanded as follows:

$$M_2(D) = \mu_1 \frac{1}{4}(1 - 2D\overline{D})T + \mu_2 T^2(\frac{D^3}{6} - \frac{D^2}{4} + \frac{D}{12}) + \mu_3 T^3(\frac{D^4}{24} - \frac{D^3}{12} + \frac{D^2}{24} - \frac{1}{48}) + \dots . \tag{50}$$

Hence, one can notice that the term $M_2(D)$ is missing in (2) or equivalently in (3) and therefore (48) is more general than (3). As a function of steady-state the duty cycle D, the term $M_1(D)$ is linear while the term $M_2(D)$ is curved and can be approximated by a parabola if the system does not contain a pole close to the switching frequency. One can observe that in this case only the first term in $M_2(D)$ is significant and it always positive regardless the value of D in the range (0,1). Nevertheless, the term $M_1(D)$ changes its sign depending on wether $D < 1/2$ or $D > 1/2$. For $D < 1/2$, the term $M_1(D)$ is negative. In this case, the system will be stable even without ramp compensation ($m_a = 0$) if $M_2(D) < -M_1(D)$. Otherwise the system will exhibit subharmonic oscillation. For duty cycle values $D > 1/2$, both $M_1(D)$ and $M_2(D)$ are positive. In this case, the system cannot be stable without using an external ramp compensator. The minimum required slope of the ramp is the sum $M_1(D) + M_2(D)$. In order to guarantee stability, any controller should be able to make the previous sum less than the used compensator slope m_a. The expressions of the terms $M_1(D)$ and $M_2(D)$ as a function of the duty cycle and the system parameters can reveal new techniques of avoiding subharmonic oscillation in switching converters. In a separate work, some alternative techniques based on this fact will be studied.

As mentioned earlier, the accuracy of the approximation up to second order term is mainly dependent on the spectral radii $sr(\mathbf{A}_1 DT)$ and $sr(\mathbf{A}_2 \overline{D}T)$ of the matrices $\mathbf{A}_1 DT$ and $\mathbf{A}_2 \overline{D}T$. Moreover, depending on the converter topology, the controller used and values of parasitic parameters, either $M_1(D)$, related to the slope of v_{con}, or $M_2(D)$, related to its ripple when the approximation up-to second order term is valid, can be dominant in predicting instability. Roughly speaking, if the waveforms of v_{con} can be approximated during switching time intervals by straight lines, the term $M_1(D)$ is dominant and $M_2(D)$ is a corrective term. On the contrary, if the waveforms of v_{con} can be approximated by parabola, the term $M_2(D)$ is dominant and $M_1(D)$ is a corrective term. In those situations where v_{con} is a combination of both straight lines and parabola, both $M_1(D)$ and $M_2(D)$ and are dominant. Table 1 summarizes the appropriate condition that should be used for different cases. For CMC without voltage feedback, v_{con} can be approximated by straight lines and (2) is accurate enough regardless of the converter topology. For CMC with voltage feedback under the condition $sr(\mathbf{A}_i \overline{D}T) \ll 1$, v_{con} is a combination of both straight lines and parabola and (18) should be used. Note that the case $\mathbf{A}_1 = \mathbf{A}_2$ in Table 1 also include those cases for which $\mathbf{B} := \mathbf{m}_1(\mathbf{x}) - \mathbf{m}_2(\mathbf{x})$ depends only on slow and practically constant state variables such as the capacitor voltage.

Table 1. The critical stability conditions for different cases.

	CMC with voltage loop open	**CMC with voltage loop closed**	**CMC with voltage loop closed and** $sr(\mathbf{A}_i\overline{D}T) \ll 1$
$\mathbf{A}_1 \neq \mathbf{A}_2$	Eq. (2)	Eq. 8, 10 or 11	Eq. 8
$\mathbf{A}_1 = \mathbf{A}_2$	Eq. (2)	Eq. 8	Eq. 8 or 22

7. Limitations of the slope and the ripple-based criteria

The ripple index is an approximated design-oriented tool which is valid under certain conditions in the same manner that the slope-based condition widely used by power electronics community is only valid under specific conditions. This is considered to be a penalty to having a simplified expression with the important advantage of being oriented to design. In general, the ripple-based index would fail when the spectral radius $sr(\mathbf{A}T)$ of the state matrix $\mathbf{A}T$ is comparable to or greater than 1. This is not a practical case. The spectral radius of the matrix $\mathbf{A}T$ in Example 1 in (Fang , 2013), which was presented as a counter-example of the ripple index hypothesis, is $r(\mathbf{A}T) = T/(RC) = 2\pi > 1$ with a non practical value of the load resistance $R = 0.01\ \Omega$. A requirement on the relationship between R, L, C and T can be found in (Cuk , 1977) where it is stated that the following two conditions must hold: $T/(RC) << 2$ and $T/\sqrt{LC} << 2\pi$. The parameter values in Example 1 in (Fang , 2013) do not only violate the necessary and sufficient condition for applying the ripple-based approach but also violate the conditions for applying the widely adopted averaged modeling approach (Erickson and Maksimovic , 2001). The generalized slope-based criterion given in (11) is valid and accurate in the general case $\mathbf{A}_1 \neq \mathbf{A}_2$ provided that the spectral radii of the matrices $\mathbf{A}_1 DT$ and $\mathbf{A}_2\overline{D}T$ are sufficiently smaller than 1. A practical case where the spectral radius $sr(\mathbf{A}_i T)$ is comparable to or greater than 1 and the ripple-based index would fail is when the controller contains a pole comparable to the switching frequency. However, even under this condition, a good estimate of the critical value of parameters can still be obtained by the simplified approach presented in (El Aroudi *et al.* , 2015-b) provided that practical values of parameters are used.

Contributions and Conclusions

In this work a new exact expression for predicting subharmonic oscillation has been presented and has been shown to be very accurate to locate the stability boundary in switching converters. This expression is then approximated by design-oriented expressions have been obtained assuming largely met practical and realistic conditions. The obtained expressions has been applied to locate instability boundaries in switching regulators under CMC. It has been demonstrated that the derived design-oriented expressions can be formulated in terms of the slopes of the control signal or its relative ripple amplitude depending on the relative degree of the total loop gain of the regulator. The analysis of this expression reveals with a relative ease the effect of each parameter upon the stability boundary. Its general-purpose applicability has been demonstrated by means of numerical simulations for different examples of switching converters under CMC with output voltage regulation.

The approach has been illustrated using different examples of switching regulators under different control strategies. The paper finally provides a discussion on design guidelines for the synthesis of new controllers for fast-scale instability as well as the limitations of the approach. For an accurate prediction using the approximate expression, switching frequency must be larger than all the filtering components in the power stage. The poles of the controllers must be far a way from the switching frequency. Under these circumstance a Taylor series expansion up to the relative degree of the driving-to-the-feedback signal transfer function will give accurate results. Current mode control is mandatory in some applications like grid connected DC-AC inverters and power factor correction AC-DC pre-regulators and it would be highly important to predict their stability limits. The major obstacle in this case is that in these systems the duty cycle is time varying within a certain interval. However, assuming a slow variation of the duty cycle, the approach presented in this paper is still applicable by making the duty cycle to follow the template dictated by the inverter or the power factor correction pre-regulator. Future work will deal with the subharmonic oscillation boundaries in this kind of applications.

References

Anunciada A. V., Silva M. M. On the stability and subharmonic susceptibility of current-mode controlled converters. *23rd Annual IEEE Power Electronics Specialists Conference, 1992.* PESC '92 Record., pp.345-353 Vol. 1, 29 Jun-3 Jul 1992.

Bianconi E., Calvente J., Giral R., Mamarelis E., Petrone G., Ramos-Paja C. A., Spagnuolo G., Vitelli M. A fast current-based MPPT technique employing sliding Mode control. *IEEE Transactions on Industrial Electronics.* Vol. 60, No. 3, pp. 1168-1178, 2012.

Chan W. C. Y., Tse C. K. Study of bifurcations in current-programmed DC-DC boost converters: from quasiperiodicity to period-doubling. *IEEE Transactions on Circuits and Systems I: Fundamental Theory and Applications*, vol. 44, No. 12, pp. 1129–1142, 1997.

Corriou J.-P. *Process control: Theory and applications.* Springer, ISBN 978-1-4471-3848-8, 2014.

Čuk S. M. *Modeling, analysis and design of switching converters.* Doctoral dissertation, California Institute of Technology, Pasadena, California, 1977.

Daly K. C. The stability of DC/DC converters in current programmed mode. *International Journal of Electronics.* Vol. 52, No. 5, 1982.

Deisch C. W. *Simple switching control method changes power converter into a current source. IEEE Power Electronics Specialists Conference, 1978 Record,* pp. 300-306, 1978.

El Aroudi A., Calvente J., Giral R., Al-Numay M., and Martinez-Salamero L. Boundaries of Subharmonic Oscillations Associated to Filtering Effects of Controllers and Current Sensors in Switched Converters Under CMC", *IEEE Transactions on Industrial Electronics.* early access, 2015.

El Aroudi A. A time-domain asymptotic approach to predict saddle-node and period doubling bifurcations in pulse width modulated piecewise linear systems. *MATEC web of Conferences. International Conference on Structural Nonlinear Dynamics and Diagnosis*, Agadir, Morocco, 2014.

El Aroudi A., Giaouris D., Iu H. H. C. and Hiskens I. A Review on Stability Analysis Methods for Switching Mode Power Converters. *IEEE Journal on Emerging Topics on Circuits and Systems*, vol.5, No. 3, pp.302-315, 2015.

El Aroudi A., Al-Numay M., Al Hosani K. and Al Sayari N. A Time-domain asymptotic approach to predict saddle-node and period doubling bifurcations in pulse width modulated piecewise linear systems. in *Structural Nonlinear Dynamics and Diagnosis, vol. 168 of the series Springer Proceedings in Physics.* pp. 367-391, 2015.

El Aroudi A. Prediction of subharmonic oscillation in switching converters under different control strategies," *IEEE Transactions on Circuits and Systems II: Express Briefs*, Vol. 62, No. 11, pp-910-914, 2014.

Erickson R. W. and Maksimovic D., *Fundamentals of power electronics*. Lluwer, 2001.

Fang C.-C., "Closed-form critical conditions of subharmonic oscillations for buck converters," *IEEE Transactions on Circuits and Systems I: Regular Papers*, Vol. 60, No. 7, pp. 1967-1974, 2013.

Fang C.-C. Instability Conditions for a Class of Switched Linear Systems With Switching Delays Based on Sampled-Data Analysis: Applications to DC-DC Converters. *Nonlinear Dynamics*, Vol. 77, No. 1, pp. 185-208, 2014.

Giaouris D., Banerjee S., Zahawi B., Pickert V. Stability Analysis of the Continuous-Conduction-Mode Buck Converter Via Filippov's Method. *IEEE Transactions on Circuits and Systems I: Regular Papers.* Vol. 55, No. 4, pp. 1084-1096, 2008.

Holland B.,"Modelling, analysis and compensation of the current-mode converter", *Proc. Powercon.* Vol. 11, No. I2-1-I-2-6, 1984.

Kabe T., Parui S., Torikai H., Banerjee S. and Saito T. Analysis of piecewise constant models of curent mode controlled DC-DC converters. *IEICE Transactions on Fundamentals of Electronics, Communication and Computer Siences*, E90-A(2), 2007, pp. 448-456.

Kapat, S., Krein P. T. Formulation of PID control for DCDC converters based on capacitor current: A geometric context. *IEEE Transactions on Power Electronics.* Vol. 27, No. 3, pp. 1424-1432, 2012.

Lee S. W. Practical feedback loop analysis for current-mode boost converter. Texas Instruments, Application Report SLVA636-March 2014, available online.

Lewin L. *Polylogarithms and associated functions.* New York, North-Holland, 1981.

Middlebrook R. D. and Čuk S. A general unified approach to modeling switching-converter power stages. *International Journal of Electronics.* Vol. 42, No. 6, pp. 521-550, 1977.

Redl R. and Novak I. Instabilities in current-mode controlled switching voltage regulators. in *IEEE Power Electronics Specialists Conference (PESC'81)*, 1981, pp. 17–28.

Ridley R. B. A new continuous-time model for current-mode control. *IEEE Transactions on Power Electronics*, vol.6, No. 2, pp. 271-282, 1991.

Rodriguez E., Guinjoan F., El Aroudi A., and Alarcon E. A ripple-based design-oriented approach for predicting fast-scale instability in DC-DC switching power supplies. *Transactions on Circuits and Systems I: Fundamental Theory and Applications*, vol. 59, No. 1, pp. 215–227, 2012.

Rodriguez E., Martinez H., Guinjoan F., Poveda A., El Aroudi A., Alarcon E. Ripple-based prediction of fast-scale instabilities in current mode controlled switching converters. *IEEE International Symposium on Circuits and Systems (ISCAS'2012)*, pp. 688-691, 20-23, 2012.

Siewniak P. and Grzesik B. A brief review of models of DCDC power electronic converters for analysis of their stability. *International Journal of Electronics.* Vol. 101, No. 10, 2014.

Singh S. P. Output ripple voltage for buck Switching regulator. Application Report SLVA630January 2014, Texas Instruments.

Tan F. D., and Middlebrook R. D. A Unified model for current-programmed converters. *IEEE Transactions on Power Electronics*, Vol. 10, No. 4 p. 397-408, 1995.

Tsai J.-F. and Chen Y.-P. Sliding mode control and stability analysis of buck DC-DC converter. *International Journal of Electronics.* Vol. 94, No. 3, pp. 209222, 2007.

Tse C. K. Flip bifurcation and chaos in three-state boost switching regulators. *IEEE Transactions on Circuits and Systems I: Fundamental Theory and Applications*, vol. 41, No. 1, pp. 16–23, 1994.